Numerical analysis of the influence of vortex on the pressure pulsation in axial flow pump system based on the CFD

X J Song and C Liu

School of Hydraulic Energy and Power Engineering, Yangzhou University, Yangzhou, Jiangsu, 225009, China

Abstract: The pressure pulsation is one of the main causes of vibration and noise in axial flow pump, in order to study the mechanism of pressure fluctuation induced by vortex, several pressure pulsation monitoring points were stalled at the bottom of the pump sump, the horn mouth, the impeller inlet and outlet, the outlet of the guide vane. The flow rate of $1.2Q_d$ (Q=38.4L/s) was selected at the speed of 2200r/min. Realizable k- epsilon turbulence model is adopted with setting up different time calculation methods by using CFX software. Changing the time step, unsteady calculation of axial flow pump device is carried out, and the pressure values of different monitoring points at different time are obtained. The frequency domain characteristics of different feature sections are obtained by FFT. The results show that the vortex position at the bottom of the inlet of the flare tube is consistent with the position of the low pressure zone, and the main frequency of the pressure fluctuation is twice of the frequency of the impeller. The characteristics of pressure fluctuation at the bottom of the inlet of the horn are consistent with the experimental results. Under the influence of impeller rotation, the main frequency of pressure fluctuation at the inlet and outlet of impeller is 4 times of the impeller rotation frequency. The main frequency of pressure fluctuation at the guide vane outlet is 3 times of that of the impeller. The amplitude of pressure fluctuation increases gradually from the bottom of inlet to the inlet of impeller. On the whole, the maximum amplitude of pressure fluctuation is at the inlet of impeller, and the maximum amplitude of pressure fluctuation occurs at the center of the vortex belt. The C_p value of the pressure fluctuation at the center of the vortex belt is about 1.8-2 times of the C_p value of the pressure fluctuation at the non-central point.

1. Introduction

Axial flow pump with the character of the large flow and the low head, widely used in irrigation and drainage pumping station and water diversion and other large-scale inter basin water diversion project. The vortex in the structure of inlet has great harm for the safe operation of the whole pump, not only led to a substantial decline in the performance of the pumps, and even cause the emergence of serious vibration and noise, seriously affect the safe and stable operation of pumping station. The vortex in the pump sump and the vortex in the flare tube affect the structure of the inner flow field and cause the pressure pulsation in the pump sump. For the study of vortex, the relationship between vortex and velocity is more studied from the structure of flow field [1-2]. The occurrence of vortex is a transient process. The factors influencing the vortex formation are complicated, and the relationship between the pressure fluctuation and the occurrence of vortex can be found, which can provide the basis for the exploration of the mechanism of vortex generation.

In this paper, in view of the study on the pressure fluctuation in the pump sump and flare tube caused by the vortex is not enough. Several pressure pulsation monitoring points were stalled at the bottom of the pump sump, the horn mouth, the impeller inlet and outlet, the outlet of the guide vane. Unsteady flow numerical simulation of full flow passage in axial flow pump unit is carried out by using CFX software with setting different time calculation method and using Realizable k-turbulence model.

2. Numerical simulation

2.1. Control equations

Based on the RANS equation, the three-dimensional unsteady flow of incompressible fluid in a axial flow pump is described. The continuity equation and momentum equation are respectively[3-5]:

$$\frac{\partial \rho}{\partial t}+\frac{\partial(\rho u_i)}{\partial x_i}=0 \tag{1}$$

$$\frac{\partial}{\partial t}(\rho u_i)+\frac{\partial}{\partial x_j}(\rho u_j u_i)=\rho F_i-\frac{\partial p}{\partial x_i}+\frac{\partial}{\partial x_j}\left(\mu\frac{\partial u_i}{x_j}\right) \tag{2}$$

Where ρ—The density of water，kg/m^3 μ—Turbulent viscosity
u_i, u_j—Time averaged velocity component
F_i—Body force p—Pressure

2.2. Turbulence model

Due to the use of Realizable k- model is no longer assumed that the turbulent kinetic energy calculation coefficient Cμ is constant, and the strain rate were established, more accurate prediction on the location and shape of the vortex. So in this paper，the Realizable k-ε turbulence model is used for the unsteady numerical simulation of the vortex flow in the pump sump. Realisable k-epsilon model [6]:

Transport Equations:

$$\frac{\partial}{\partial t}(\rho k)+\frac{\partial}{\partial x_j}(\rho k u_j)=\frac{\partial}{\partial x_j}\left[\left(\mu+\frac{\mu_t}{\sigma_k}\right)\frac{\partial k}{\partial x_j}\right]+P_k+P_b-\rho\varepsilon-Y_M+S_k \tag{3}$$

$$\frac{\partial}{\partial t}(\rho\varepsilon)+\frac{\partial}{\partial x_j}(\rho\varepsilon u_j)=\frac{\partial}{\partial x_j}\left[\left(\mu+\frac{\mu_t}{\sigma_\varepsilon}\right)\frac{\partial \varepsilon}{\partial x_j}\right]+\rho C_1 S_\varepsilon-\rho C_2\frac{\varepsilon^2}{k+\sqrt{\nu\varepsilon}}+C_{1\varepsilon}\frac{\varepsilon}{k}C_{3\varepsilon}P_b+S_\varepsilon \tag{4}$$

Where

$$C_1=max\left[0.43,\frac{\eta}{\eta+5}\right],\quad \eta=S\frac{k}{\varepsilon},\quad S=\sqrt{2S_{ij}S_{ij}} \tag{5}$$

In these equations, P_k represents the generation of turbulence kinetic energy due to the mean velocity gradients, calculated in same manner as standard k-epsilon model.P_b is the generation of turbulence kinetic energy due to buoyancy, calculated in same way as standard k-epsilon model.

Modelling turbulent viscosity:

$$\mu_t = \rho C_\mu \frac{k^2}{\varepsilon} \tag{6}$$

Where

$$C_\mu = \frac{1}{A_0 + A_s \frac{kU^*}{\varepsilon}}, \quad U^* \equiv \sqrt{S_{ij}S_{ij} + \overline{\Omega}_{ij}\overline{\Omega}_{ij}}, \quad \overline{\Omega}_{ij} = \Omega_{ij} - 2\varepsilon_{ijk}\omega_k \text{ and } \Omega_{ij} = \overline{\Omega}_{ij} - \varepsilon_{ijk}\omega_k \tag{7}$$

Where

$\overline{\Omega}$ is the mean rate-of-rotation tensor viewed in a rotating reference frame with the angular velocity ω. The model constants A_0 and A_s are given by:

A_0=4.04，$A_s = \sqrt{6}\cos Ø$，$Ø = \frac{1}{3}\cos^{-1}(\sqrt{6}W)$，$W = \frac{S_{ij}S_{jk}S_{ki}}{\overline{S}^3}$，$\overline{S} = \sqrt{S_{ij}S_{ij}}$，$S_{ij} = \frac{1}{2}\left(\frac{\partial u_j}{\partial x_i} + \frac{\partial u_i}{\partial x_j}\right)$

Model constants：$C_{1\epsilon}$=1.44，C_2=1.9, σ_k=1.0, σ_ϵ=1.2

2.3. Calculation model and mesh

The study object of this article is the 120mm vertical axial flow pump device, as shown in figure 1. The impeller diameter is 120mm, the tip clearance is 0.1mm, the wheel diameter is 48mm, the number of leaves is 4, the blade angle is 0°, the guide vane number is 7. The unstructured mesh of the calculation model is generated by using Workbench software. Because of the complexity of the flow region near the flare tube, this region of the mesh refinement, the mesh quality is greater than 0.6, the total number of grid of the unit reached 2 million 500 thousand, that can meet the precision requirements of numerical calculation.

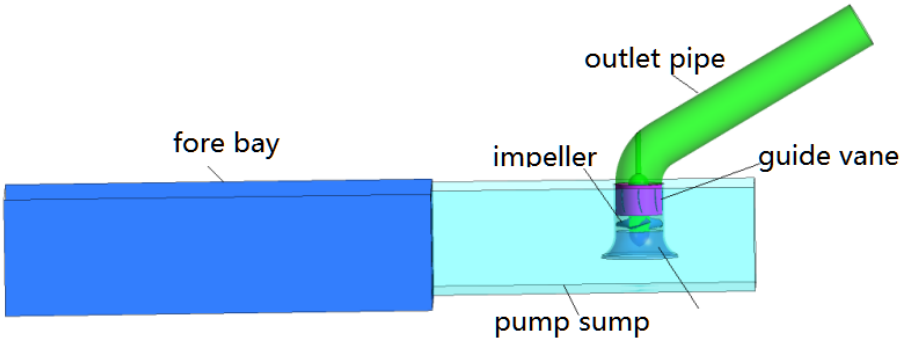

Figure 1. The vertical axial flow pump model diagram.

2.4. Boundary conditions and solution method

In ANSYS CFX Pre-treatment, import condition is set as mass flow inlet conditions, the export condition is set as the average static pressure conditions that is 1atm, the free surface is set as symmetrical plane boundary type without considering the surface wave, the wall boundary type is set as a non-slip sidewall [7-8].

By using different time step coefficients that the Timescale factor are 1, 1.1, 1.2, 5, 10 respectively in steady calculation, compared with the experimental results, it is found that when the Timescale factor=1.2 the results are closer to the experimental results [9]. In order to make the unsteady calculation result more accurate, the unsteady calculation is carried out on the results of steady calculation, and the monitoring points on different sections are selected in the unsteady calculation, as shown in figure 2. The vortex is a transient process, so in order to get the vortex numerical calculation result calculate, the total setting time is set as 10 rotation period of the impeller. Since the pressure fluctuation in the first two rotation period of the impeller is unstable, the pressure fluctuation data of the latter 8 rotation period of the impeller were analyzed.

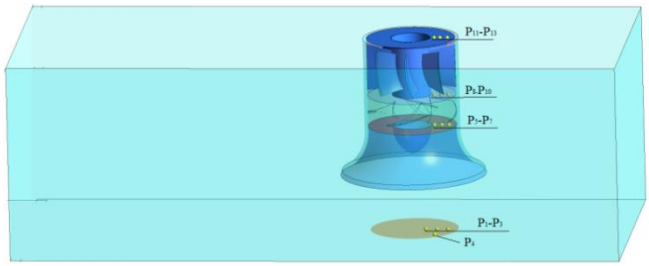

Figure 2. Position diagram of pressure fluctuation monitoring points at different sections.

3. Result Analysis

3.1. Reliability analysis of numerical simulation results

The pressure fluctuation characteristics and pressure distribution at the bottom of the pump sump are obtained by CFD numerical simulation, and compared to model experiment results to verify the reliability of the numerical simulation results [10-11]. The position the vortex at the bottom of the pump sump are shown in figure3. The numerical simulation result of the pressure distribution and the experiment result the pressure distribution at the bottom of the pump sump below the flare tube under the large flow condition are shown in Figure4, that can determine the numerical simulation results is basically consistent with experimental results. The frequency characteristic results of the pressure pulsation at the bottom of the pump sump below the flare tube obtained by the numerical simulation and the model experiment under large flow condition are shown in Figure5. It is found that the main frequency of the pressure pulsation at the bottom of the pump sump below the flare tube is 2 times of the impeller rotation frequency. The results show that the percentage error between the model experiment and the numerical simulation is not more than 10%. So it can determine that the calculation model is reliable.

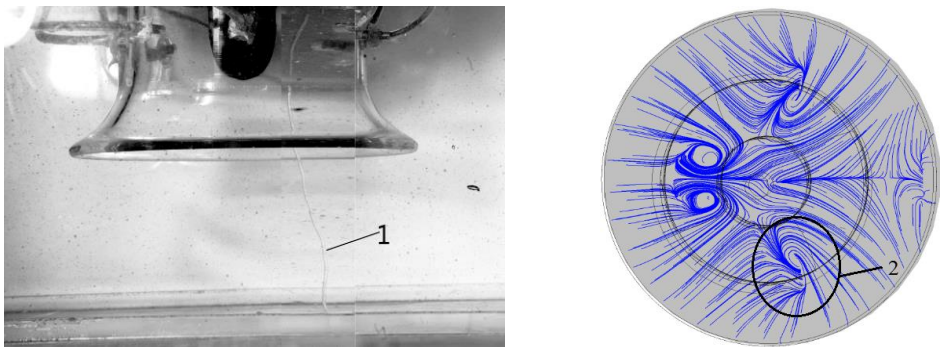

(a) Model test result (b) Numerical simulation results

Figure 3. The position the vortex at the bottom of the pump sump.

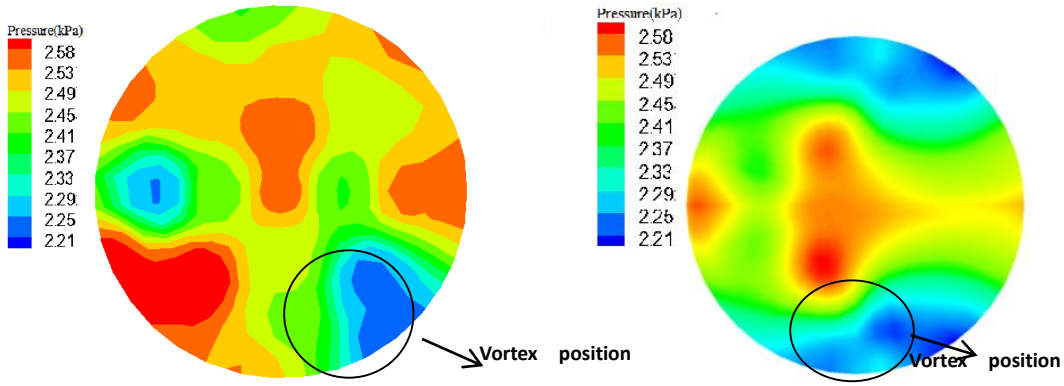

(a) Model test result (b) Numerical simulation results

Figure 4. The pressure distribution at the bottom of the pump sump below the flare tube.

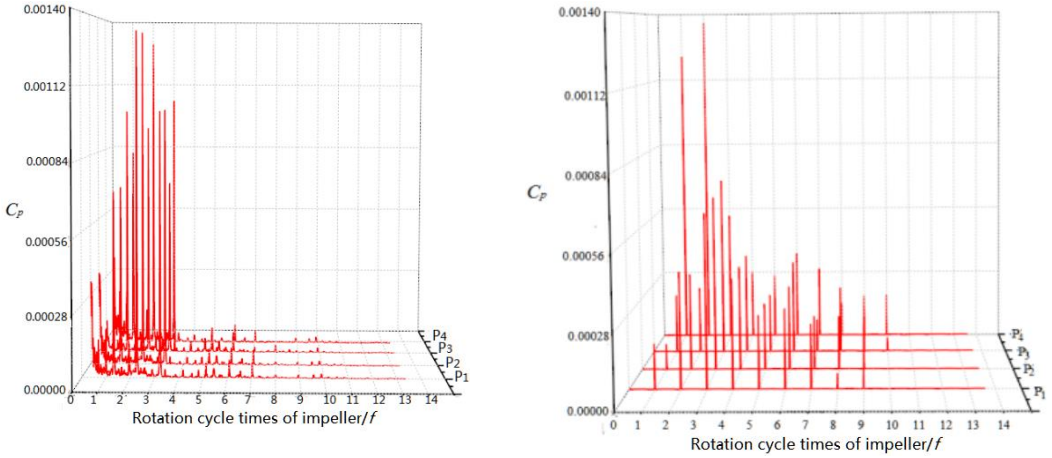

(a) Model test result (b) Numerical simulation results

Figure 5. Frequency - domain diagram of the pressure fluctuation at the bottom of the pump sump below the flare tube.

3.2. Analysis of the frequency domain of the pressure fluctuation

The pressure fluctuation data is transformed by FFT[12-15], and the frequency characteristic curve of pressure pulsation at different measuring sections is obtained by software Origin9.0.The amplitude of pressure fluctuation is expressed by C_p[16-17].

3.2.1. At the bottom of the pump sump. As shown in figure 5, by comparing the experiment results and the numerical simulation results of the pressure fluctuation at the bottom of the pump sump below the flare tube that can determine the main frequency of the pressure pulsation is 2 times of the impeller rotation frequency. The maximum values C_p of the pressure fluctuation of the measuring points P1, P2 and P3 at the bottom of the pump sump below the flare tube obtained by the CFD respectively are 0.00066, 0.000683, 0.000715. The center of the vortex is at the position of measuring point P20 that the amplitude of pressure pulsation in the measuring point P4 is the largest whose the Cp value is 0.00136. At the center of the vortex, the Cp value of the measuring point P4 at 1 octave of the impeller rotation frequency is 0.00122. The C_p value of the pressure fluctuation at the center of the vortex belt is about 1.8-2 times of the C_p value of the pressure fluctuation at the non-central point. This shows that there is an obvious pressure gradient in the vortex, which results in a great pressure fluctuation in center zone of the vortex. According to the pressure fluctuation at the center of the vortex belt, the pressure fluctuation amplitude at the 1 octave is large, and the

pressure fluctuation in the center zone of the vortex is more complex and frequent. There is obvious harmonic fluctuation at the center of vortex belt, which indicates that the change of the vortex will cause obvious pressure fluctuations. In the initial stage of the vortex, a large pressure gradient has formed around the vortex belt. The formation and disappearance of the vortex affect the variation of pressure around the flare tube all the time.

3.2.2. At the inlet of the pump impeller. The frequency characteristic curve of the pressure pulsation of the measuring points P5~P7 in the impeller inlet is shown in figure6. At 1 octave of the impeller rotation frequency and 4 times of the impeller rotation frequency, the pressure has obvious fluctuations, the main frequency of the pressure pulsation is 4 times of the impeller rotation frequency that equals the blade frequency of the impeller. The C_p of the main frequency of the pressure pulsation at the measuring points P5~P7 in the impeller inlet respectively are 0.000965, 0.000836, 0.000847, that shows the pressure pulsation of the impeller inlet is directly influenced by the rotation of the impeller. There exist great fluctuations at 1 octave of the impeller rotation frequency at the impeller inlet that is synchronous with the pressure fluctuation at the vortex center occurring at the 1octave of the impeller rotation frequency below the flare tube.

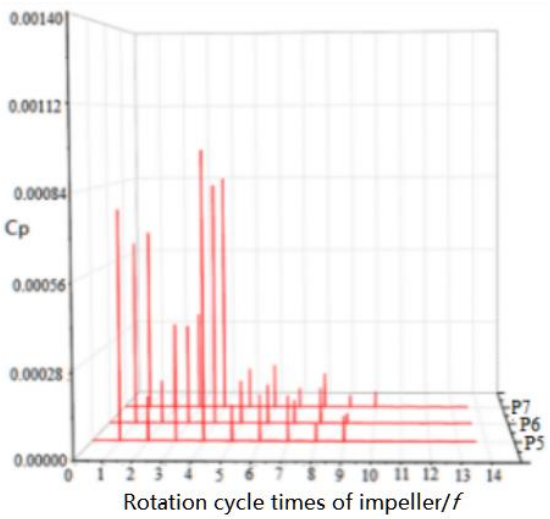

(c) Impeller inlet

Figure 6. Frequency - domain diagram of the pressure fluctuation at the impeller inlet.

3.2.3. At the outlet of the pump impeller. The frequency characteristic curve of the pressure pulsation of the measuring pointsP8-P10 at the impeller outlet is shown in figure 7. Under the influence of impeller rotation, the main frequency of pressure pulsation at the impeller outlet is 4 times of that of the impeller rotating frequency that is the frequency of the blade. The maximum values C_p of the pressure fluctuation of the measuring points P8, P9andP10 respectively are 0.000829, 0.000867 and 0.000861. At 3 times of the impeller rotation frequency at the impeller outlet, the Cp values of the pressure fluctuation at the impeller frequency are 0.000500, 0.000622, and 0.000229. What is different from the pressure fluctuation at the impeller inlet is that the secondary frequency of pressure fluctuation at the impeller outlet is mainly concentrated at 3 times of the impeller frequency, which is due to the rotor-stator interaction between the impeller and the guide vanes. The guide vanes and the impeller are the excitation source, which leads to the harmonics except the impeller rotation. Inside the impeller, due to the rotation of the impeller, the pressure fluctuation caused by the vortex has been attenuated, so the harmonic wave at 1 octave of the rotation frequency is obviously reduced. In a word, the pressure pulsation at impeller outlet is mainly influenced by the rotation of

the impeller.

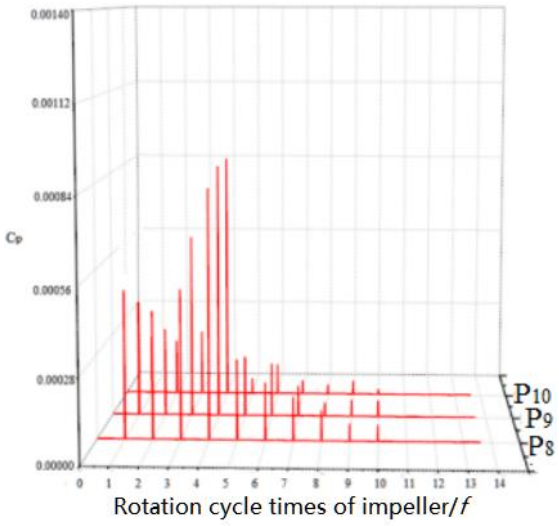

(d) Impeller outlet

Figure 7. Frequency - domain diagram of the pressure fluctuation at the impeller outlet.

3.2.4. At the outlet of the guide vane. The frequency domain characteristic diagram of the pressure pulsation at the measuring points P11, P12andP13 at the guide vane outlet is shown in figure 8. After the rectification, the main frequency of pressure pulsation at the guide vane outlet is 3 times of the impeller rotation frequency, and The maximum values C_p of the pressure fluctuation at the measuring points P11,P12andP13respectively are 0.000815,0.000970and 0.000582.The pressure fluctuation at the inside of the guide vane is also influenced by the rotor-stator interaction between the impeller and the guide vanes, that the impeller rotation is the excitation source for the pressure pulsation in the guide vane inside .

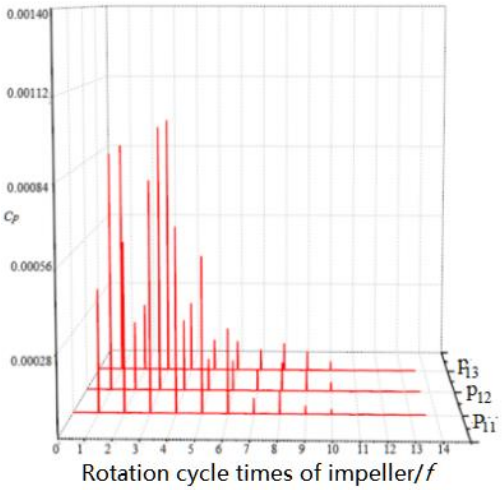

(e) Guide vane outlet

Figure 8. Frequency - domain diagram of the pressure fluctuation at the guide vane outlet.

The frequency domain characteristics of pressure pulsation in the different sections from the bottom of the pump sump to the outlet of the guide vane are compared. Can be found, the pressure pulsation amplitude at the impeller inlet is larger than that in other sections on the whole, but the maximum amplitude of pressure pulsation is in the center of the vortex, which indicates that the pressure fluctuation caused by vortex is dominant below the flare tube. According to the principle of vibration, under the large flow conditions, the main frequency amplitude of the pressure fluctuation caused by the vortex is small, and once it is close to the natural frequency of the pump device, that may lead to the resonance of the pump device.

3.3. Pressure distribution

In order to investigate the pressure changes in the water pump caused by the pressure fluctuation, different characteristic sections starting from the bottom of the pump sump below the flare tube along the Z direction are taken, section layout as shown in figure 9. The distance of the section1-1, 2-2 from the bottom of the pump sump respectively are 3mm, 28mm.The 3-3 section is the inlet section of the flare tube, the 4-4 section is the inlet section of the impeller, the 5-5 section is the outlet section of the impeller, and the 6-6 section is the outlet section of the guide vane. The pressure distribution of each feature section is analyzed, under the large flow condition, the pressure distribution from the bottom of the pump sump to the exit of the guide vane is shown in figure 10.

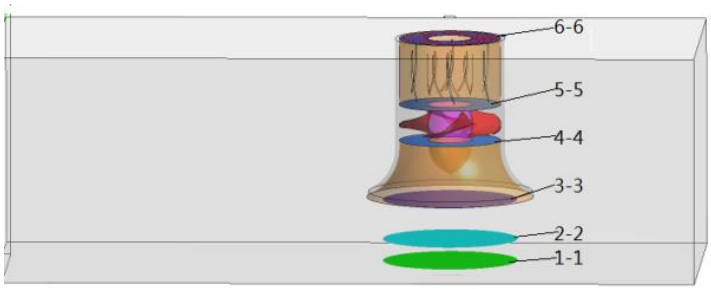

Figure 9. Different characteristic section of the pressure distribution.

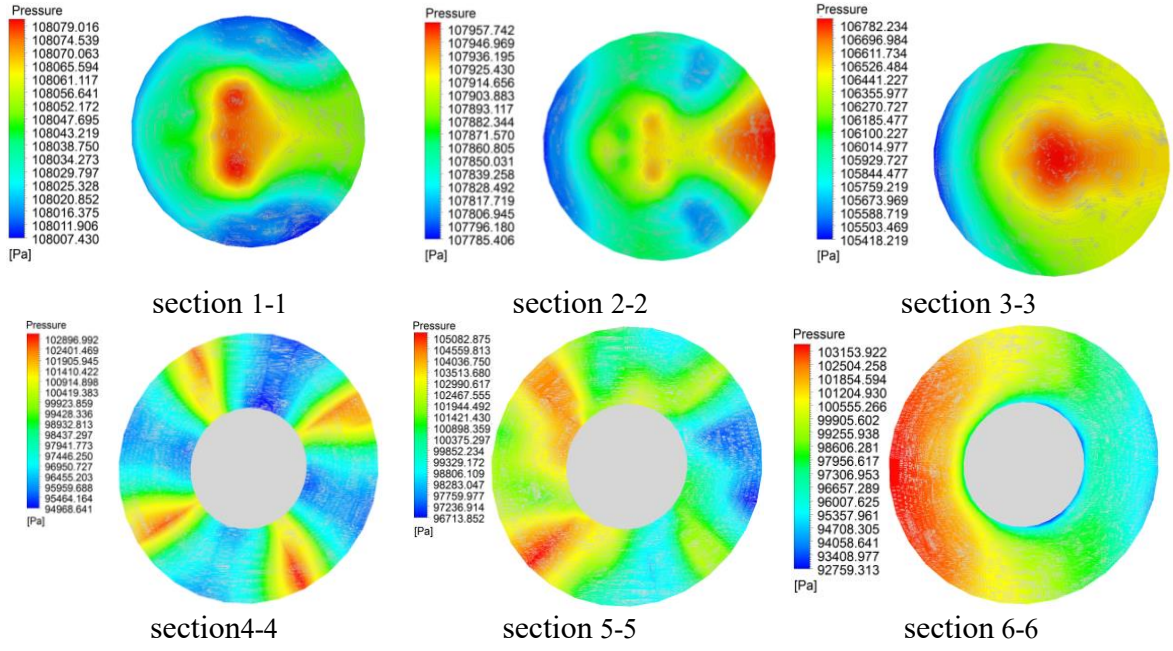

Figure10. Pressure distribution at different sections

Under the flare tube, there is a low pressure area in the right rear position corresponding to position of the vortex tube, and the pressure distribution of the 1-1 section and the 2-2 section is similar. Relative to the low pressure area in the 2-2 section, the area of the low pressure area at the tail of the vortex tube is larger. Along the direction of the vortex tube developing upward, the vortex tube becomes thinner, and the area of the low pressure area near the vortex tube becomes smaller, and accompany with the vortex going into the flare tube that disappears gradually. It can be seen from the pressure contour of the 3-3 section that the influence of the vortex on the pressure decreases with the decrease of the vortex intensity at the moment when the vortex enters the flare tube. The pressure distribution of 4-4 section and 5-5 section have some similarity, but the impeller inlet pressure is mainly affected by the rotation of the impeller, the pressure distribution is alternately distributed with the high pressure and low pressure areas that corresponding to the number of blades. The pressure distribution of impeller outlet is also affected by the rotation of the impeller that is also alternately distributed with the high pressure and low pressure areas that corresponding to the number of blades. But the rotor-stator interaction between the impeller and the guide vanes lead to the pressure distribution at the impeller outlet having changed and the pressure on the left side of the impeller is higher than that on the right.

On the whole, the pressure is gradually reduced from the bottom of pump sump to the inlet of the impeller, and the pressure of the impeller inlet is the minimum. The pressure from the impeller inlet to the guide vane outlet increases first and then decreases.

4. Conclusion

- As a whole, the amplitude of pressure pulsation at the inlet of the axial impeller is the very large, and the main frequency of the pressure fluctuation at the inlet and outlet of the impeller is the frequency of the impeller blade. The maximum amplitude of pressure fluctuation occurs at the center of the vortex belt, and The Cp value of the pressure fluctuation at the center of the vortex belt is about 1.8-2 times of the Cp value of the pressure fluctuation at the non-central point.
- At 1 octave of the rotation frequency, there is a pulsating harmonic between the impeller inside and the position of the vortex below the flare tube, that the vortex extends to the impeller inlet from the flare tube below and affects the pressure variation inside the impeller. Under the large flow conditions, the frequency of pressure fluctuations caused by the vortex is the low frequency, and once the low frequency is close to the natural frequency of the pump device, it may cause the pump device to resonate.
- The pressure is gradually reduced from the bottom of pump sump to the inlet of the impeller, and the pressure of the impeller inlet is the minimum. The pressure from the impeller inlet to the guide vane outlet increases first and then decreases.

Reference

[1] Liu Chao. Researches and Developments of Axial-flow Pump System [J] Transactions of the Chinese Society for Agricultural Machinery, 2015, 46(6): 49-59.
[2] He Yun. Main advances of research on vortices in pump sumps [J] Journal of Hydroelectric Engineering, 23(5):92-96.
[3] Shi Weidong, Leng Hongfei, Zhang Desheng, etal. Performance Prediction and Experiment for Pressure Fluctuation of Interior Flow in Axial-flow Pump [J] Transactions of the Chinese Society for Agricultural Machinery, 2011,42(5):44-48.
[4] Liu Chao, Cheng Li, Zhou Jiren, et al. Numerical Simulation of Three-dimensional Turbulent Flow for Opening Pump Sump[J]Transactions of the Chinese Society for Agricultural Machinery, 2002,33(6):53-55.
[5] Cong Guohui, Wang Fujun. Applicability of turbulence models in numerical simulation of vortex flow in pump sump[J]. Transactions of the CSAE, 2008,24(6:31－35.

[6] Yang Fan, Liu Chao, Tang Fangping, et al. Analysis of hydraulic performance for vertical axial-flow pumping system withcube-type inlet passage[J]. Transactions of the Chinese Society of Agricultural Engineering,2014, 30(4): 62－69.
[7] Cheng Li1, Liu Chao, Zhou Jiren. Numerical simulation of flow in the outlet passages of reversible pumping station by RNG k-E turbulent model with wall function law[J] Advances in Water Science，2004,15(1):109-112.
[8] Liu Chao, Liang Haojie, Jin Yan, etal.PIV Measurements of Intake Flow Field in Axial-flow Pump[J] Transactions of the Chinese Society for Agricultural Machinery, 2015,46(8):33-41.
[9] Yang Fan，Jin Yan，Liu Chao，et al． Numerical analysis and performance test on diving tubular pumping system with symmetric aerofoil blade［J］． Transactions of the CSAE，2012，28(16) : 60 － 67.
[10] Shinji Ebara, Hiroyuki Takamura, Hidetoshi Hashizume et al..Characteristics of Flow Field and Pressure Fluctuation in Complex Turbulent Flow in the Third Elbow of a Triple Elbow Piping with Small Curvature Radius in Three-dimensional Layout[J]. International Journal of Hydrogen Energy, 2016
[11] Arndt N, Acosta A J, Brennen C E, et al． Experimental investigation of rotor-stator interaction in a centrifugal pump with several vaned diffusers[J]. ASME Journal of Turbomachinery，1990，112(1): 98 -108．
[12] Arndt N，Acosta A J，Brennen C E，et al.Rotor-stator interaction in a diffuser pump[J].ASME Journal of Turbomachinery，1989，111(3) : 213 － 221．
[13] Zhang Desheng, Wang Haiyu, Shi Weidong, etal. Experimental Investigation of Pressure Fluctuation with Multiple Flow Rates in Scaled Axial Flow Pump[J] Transactions of the Chinese Society for Agricultural Machinery, 2014,45(11):139-144.
[14] Wang Fujun, Zhang Ling, Zhang Zhimin, etal Analysis on pressure fluctuation of unsteady flow in axial-flow pump[J]Journal of Hydraulic Engineering, 2007,38(8):1003-1009
[15] Huang Huanming, GaoHong, ShenFeng, etal.Numerical simulation and experimental validation of the flow field in axial flow pump[J] .Transactions of the Chinese Society for Agricultural Machinery, 2008, 39 (8):66 ~69.
[16] Yao Jie, Shi Weidong, Wu Suqing, et al.Numerical calculation and experiment on pressure fluctuation in axial flow pump[J].Transactions of the Chinese Society for Agricultural Machinery，2013，44(Supp． 1) : 119-124.
[17] Zhang Desheng, Shi Weidong, Zhang Hua, et al.Application of different turbulence model for predicting performance of axial flow pump[J].Transactions of the CSAE，2012，28(1) : 66 － 70.